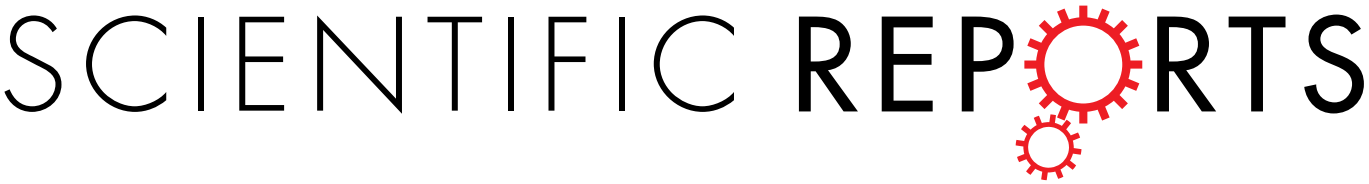

OPEN

Sensitivity of chemical weathering and dissolved carbon dynamics to hydrological conditions in a typical karst river

Received: 05 October 2016
Accepted: 17 January 2017
Published: 21 February 2017

Jun Zhong[1,2], Si-liang Li[3,4], Faxiang Tao[1], Fujun Yue[1] & Cong-Qiang Liu[1]

To better understand the mechanisms that hydrological conditions control chemical weathering and carbon dynamics in the large rivers, we investigated hydrochemistry and carbon isotopic compositions of dissolved inorganic carbon (DIC) based on high-frequency sampling in the Wujiang River draining the carbonate area in southwestern China. Concentrations of major dissolved solute do not strictly follow the dilution process with increasing discharge, and biogeochemical processes lead to variability in the concentration-discharge relationships. Temporal variations of dissolved solutes are closely related to weathering characteristics and hydrological conditions in the rainy seasons. The concentrations of dissolved carbon and the carbon isotopic compositions vary with discharge changes, suggesting that hydrological conditions and biogeochemical processes control dissolved carbon dynamics. Biological CO_2 discharge and intense carbonate weathering by soil CO_2 should be responsible for the carbon variability under various hydrological conditions during the high-flow season. The concentration of DIC_{bio} (DIC from biological sources) derived from a mixing model increases with increasing discharge, indicating that DIC_{bio} influx is the main driver of the chemostatic behaviors of riverine DIC in this typical karst river. The study highlights the sensitivity of chemical weathering and carbon dynamics to hydrological conditions in the riverine system.

Rivers play a crucial role in biogeochemical processes involved in the global carbon cycle, which link major carbon reservoirs, including atmosphere, biosphere, terrestrial geosphere, and oceans[1]. Chemical weathering is a fundamental geochemical process regulating the atmosphere-land-ocean fluxes and the climate on earth[2,3]. Forward and inverse models have been used for studying chemical weathering and CO_2 consumption in many rivers around the world[4–7]. Many studies have focused on the chemical weathering and CO_2 consumption in carbonate-rich catchments[8–10], however, few of them have investigated the temporal dynamics of stream chemistry based on long term and high frequency sampling campaigns[11], especially in carbonate-rich areas[12,13]. Carbonate weathering is highly sensitive to human activities and climate change[2,14–18], the latter of which may partly be controlled by local hydrology[14]. Understanding the dynamics of the major dissolved solutes is useful for characterizing chemical weathering in rivers[11,16]. The feedback between hydrological conditions and chemical weathering is hypothesized to play a crucial role in modulating CO_2 concentrations in carbonate-rich areas. Thus, time series observations are critical to better constrain the chemical fluxes, chemical weathering rates and the processes controlling the fate of chemical species in rivers[14,19,20].

The annual fluvial carbon flux to the oceans is estimated to be 1 Pg C/y (0.8–1.2Pg C/y), of which 38% is in the form of dissolved inorganic carbon (DIC) and 25% is in the form of dissolved organic carbon (DOC)[21,22], the rest is in the form of particulate carbon. The recognition that the carbon in inland rivers could be a substantial component in regional or global carbon budgets, has led to increased momentum in riverine biogeochemistry studies[23]. However, the patchy global estimates have been poorly constrained with respect to hydrological conditions, anthropogenic activities, acid rain etc.[22,24–26]. Riverine DIC and DOC concentrations are often, closely, associated

[1]The State Key Laboratory of Environmental Geochemistry, Institute of Geochemistry, Chinese Academy of Sciences, Guiyang 550081, China. [2]University of Chinese Academy of Sciences, Beijing 100049, China. [3]Institute of Surface-Earth System Science, Tianjin University, Tianjin 300072, China. [4]State Key laboratory of Hydraulic Engineering Simulation and Safety, Tianjin University, Tianjin 300072, China. Correspondence and requests for materials should be addressed to S.-l.L. (email: siliang.li@tju.edu.cn)

with variations in hydrology[27,28], as well as variations in sources and fluxes of dissolved carbon[26,29]. Detailed information on dissolved carbon dynamics with respect to hydrological conditions is still scarce, and relevant controlling processes are largely unknown. To constrain the DIC sources and clarify the relative biogeochemical processes, carbon isotopes can be used to identify the carbon sources and carbon biogeochemical processes[26,30–32].

The continuous exposure of carbonate rocks on the Yunnan-Guizhou plateau is the largest karst area in the world[8,10,25,26]. The Wujiang River as one of the largest rivers in the Yunnan-Guizhou plateau is an ideal river to study the chemical weathering and carbon dynamics in the carbonate-rich areas[8–10]. A series of field campaigns have been conducted to sample river water under different hydrological conditions. This study uses data collected through the field campaigns to investigate correlations among chemical weathering, dissolved carbon dynamics, biogeochemical processes and hydrology. Carbon isotopes of dissolved inorganic carbon denoted as $\delta^{13}C_{DIC}$, are used to identify carbon sources and constrain their contributions, which can provide insights into the main factors controlling carbon dynamics over time.

Results

Hydrochemical characteristics. pH of the river water samples is mildly alkaline (7.93–8.30) within the range of the whole Wujiang basin (7.6 to 8.9)[8]. The electrical conductivity (EC) values range from 315 to 407 μS/cm for the whole hydrological year (Table S1). Mean discharge-weighted concentrations can be calculated as $\Sigma(Q_iC_i)/\Sigma Q_i$, where the subscript i represents each sample during the hydrological year[33]. The total dissolved solids (TDS) range from 239 to 356 mg/L (Table S1), with an average of 265 mg/L, which is higher than the world average value (97 mg/L)[22]. In comparison to rivers draining carbonate terrain worldwide, the average TDS value of the Wujiang River is higher than that of the South Han River (174 mg/L) in South Korea[34], the Ganges and Indus rivers (164 mg/L) draining the Himalayas[35,36] and the Mackenzie River (160 mg/L) draining the Rocky Mountains[37]. However, the TDS values are in the same range with that of the upper Yellow River (274 mg/L)[7], the upper Xijiang River (297 mg/L)[25] but lower than that of the Houzhai River (441 mg/L)[26] in China. The total cationic charge ($TZ^+ = Na^+ + K^+ + 2Ca^{2+} + 2Mg^{2+}$, in μeq/L) and total dissolved anions ($TZ^- = Cl^- + 2SO_4^{2-} + HCO_3^- + NO_3^-$, in μeq/L) are well balanced, indicating that the unanalyzed ions play a minor role in charge balance. The mean discharge-weighted concentrations of major cations are as follows: Ca^{2+}(1.33 mmol/L) > Mg^{2+}(0.40 mmol/L) > Na^+(0.17 mmol/L) > K^+(0.04 mmol/L) (Fig. S1). The mean discharge-weighted concentrations of major anions are as follows: HCO_3^- (2.37 mmol/L) > SO_4^{2-} (0.44 mmol/L) > Cl^- (0.13 mmol/L) (Fig. S1). The Wujiang River shows a dominance of Ca^{2+}, Mg^{2+}, HCO_3^- and SO_4^{2-}, which is similar to the characteristics of rivers draining karst areas[10,20,36,37].

Carbon characteristics. DIC is the sum of CO_2 (aq), carbonic acid (H_2CO_3), HCO_3^-, and carbonate (CO_3^{2-}) ions[26]. The DIC concentrations in the river water vary from 2303 to 2783 μmol/L (Table S2), which is triple times higher than the world average concentration (852 μmol/L)[19]. The dissolved organic carbon (DOC) has a narrow range from 0.89 mg/L to 1.32 mg/L (Table S2), with no significant temporal variations. The partial pressure of carbon dioxide (pCO_2) is a function of respiration, which can lead to increases in both riverine pCO_2 and the dissolution of carbonate[26]. The pCO_2 values range from 711 μatm to 1619 μatm (Table S2), which is much higher than the local atmospheric pCO_2 (349 μatm) (Eq. S1). The value of $\delta^{13}C_{DIC}$ ranges from −14.8‰ in the high-flow season to −9.4‰ in the low-flow season (Table S2), with the average value of −12.1‰.

Temporal variations in major elements. The concentrations of major elements show significant temporal variations in the Wujiang River (Fig. S2). The discharge (Q) is low and relatively stable from November 2013 to March 2014 and relatively high from April 2014 to October 2014, reaching a maximum in July 2014 (Fig. S2). Generally, all the major elements (except Si) exhibit slightly decreasing trends during the high-flow season due to dilution and reach the maxima in February and March during the low-discharge period (Fig. S2). However, Si shows an increasing trend in the high-flow season relative to the low-flow season (Fig. S2).

Relationship between elemental concentrations and discharge. Godsey *et al.*[33] and Clow and Mast[38] have demonstrated that the concentrations of weathering products are negatively correlated with discharge and can be approximated as power-law functions:

$$\text{Concentration}(C) = a \times (\text{Discharge}(Q))^b$$

where a is a constant, and b represents the index that explains the deviation from chemostatic behavior[39].

The regression coefficient b in the relationship between C and Q has a physical interpretation. If $b = 0$, the catchment behaves entire chemostatically; and if $b = -1$, Q is the only controller on C, constant solute fluxes being diluted by variable fluxes of water[27]. However, when $b > 0$, no dilution effect is present, because large amounts of inputs are induced by high discharge. Significant relationships (R^2 values ranging from 0.35 to 0.65) between C and Q were found for the Wujiang River (Fig. 1). The slope values suggest that nearly all dissolved solutes (except Si) become diluted with increasing discharge and that the concentrations of Ca^{2+}, $Mg^{2+}$and HCO_3^- do not vary as much as those of Na^+, K^+, SO_4^{2-} and Cl^- (Fig. 1). Although all these dissolved solutes except Si decrease with increasing discharge, they do not strictly follow the theoretical dilution curve. Godsey *et al.*[33] have postulated that concentrations are relatively constant in wide ranges of discharge, which maybe due to large amount of water stored in a catchment flows into the river induced by intense precipitation. Matrix porosity is widely distributed in the carbonate-rich areas, which stored large amount of "old" water. The near chemostatic behavior in the catchment may be ascribed to the carbonate-rich characteristics. The concentration of Si has a positive relationship with discharge (Fig. 1), indicating that Si is not affected by dilution, and that multiple biogeochemical processes counteract the dilution effect.

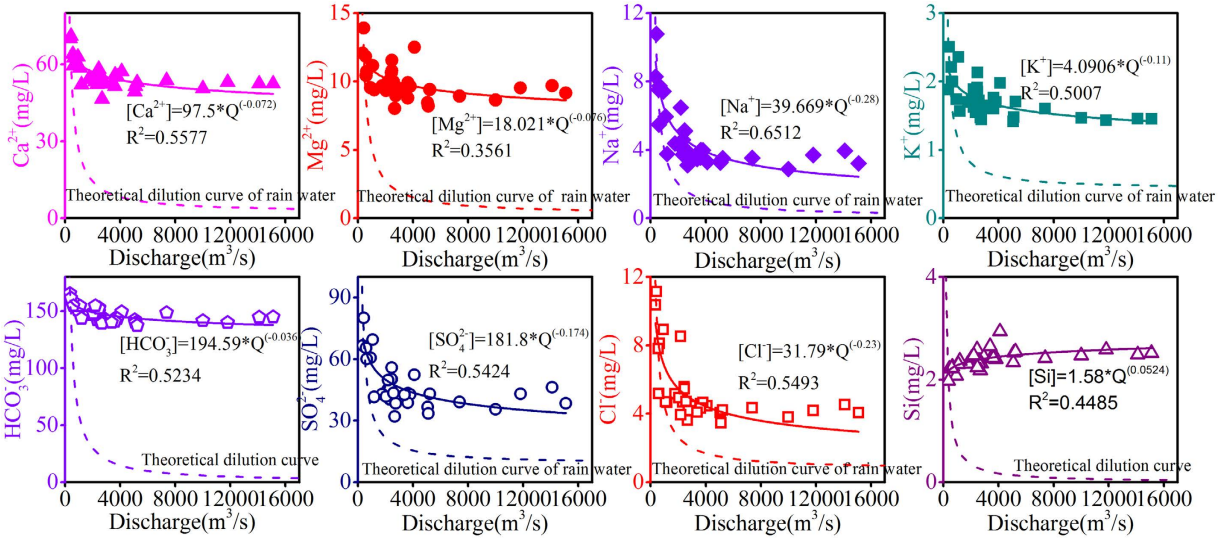

Figure 1. Concentration-discharge relationships of major elements (Ca^{2+}, Mg^{2+}, Na^{+}, K^{+}, HCO_3^{-}, SO_4^{2-}, Cl^{-}, Si). The theoretical dilution curve means that these elements are diluted by deionized water (b = −1), and the theoretical dilution curve of rain water means that these elements are diluted by rain water, which is calculated by rainwater of Guiyang.

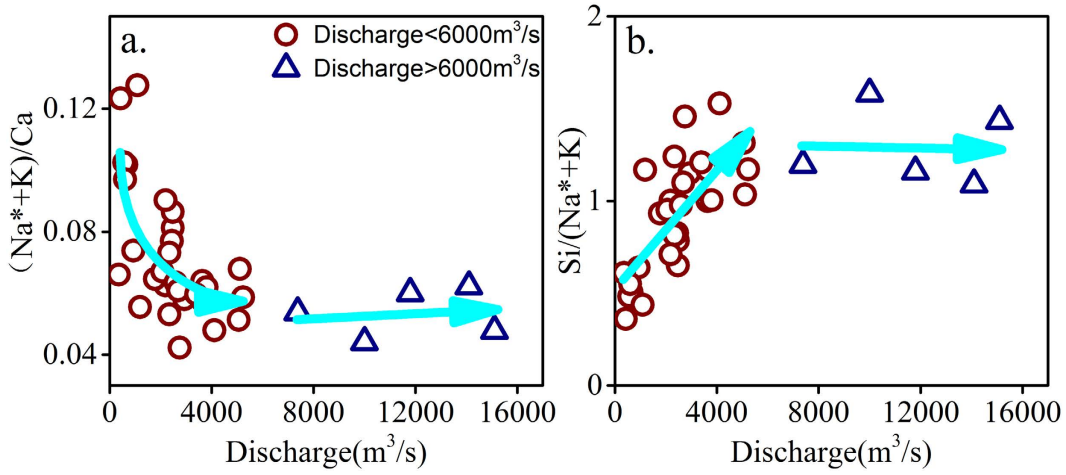

Figure 2. (**a**) Correlation between (Na* + K)/Ca ratio and discharge for the Wujiang River. (**b**) Correlation between Si/(Na* + K) ratio and discharge for the Wujiang River.

Discussion

Elemental ratio-discharge relationship. The dissolved loads of the river water are derived from atmosphere, rock weathering and anthropogenic pollutions[40]. The chemistry of river water in the Wujiang River is dominated by carbonate weathering (limestone and dolomite) (Fig. S3a). All of the samples have $[Na^+]/[Cl^-]$ ratios exceeding 1 (Fig. S3b), indicating that silicate weathering is a clear source of major ions. There is no geological evidence for the exposure of evaporites in the river basin[8], the contribution from evaporites is thus neglected. During carbonate weathering, the cations $Ca^{2+}$and $Mg^{2+}$are released into the dissolved phase. During silicate weathering, the cations Na^+, K^+, Ca^{2+} and Mg^{2+}as well as Si, are released into the dissolved phase. Carbonate weathering is the primary sources of Ca^{2+}, Mg^{2+} and HCO_3^-, and silicate weathering is the major source of Na^+, K^+ and Si in the basin[8]. Cl^- has two major sources: atmospheric and anthropogenic inputs[8]. Changes in DOC concentrations can be ascribed to mixing of multiple sources and biogeochemical processes[41].

Elemental ratio-discharge relationships can be used to identify source changes and examine biogeochemical processes during various hydrological conditions[16]. Changes in elemental ratios are related to changes in the source or differential dissolution/precipitation rates between minerals, especially for carbonate and silicate minerals, with changing discharge[14,16]. As weathering progresses, saturation with respect to secondary silicate and the retention of silicate in the reservoir can buffer the concentration of dissolved Si, while the concentrations of dissolved cations that are not readily partitioned into secondary silicates continue to increase[16,42]. The variation in the ratio of (Na* + K)/Ca ($Na^* = [Na^+] - [Cl^-]$) with changing discharge (Fig. 2a) suggests that the relative

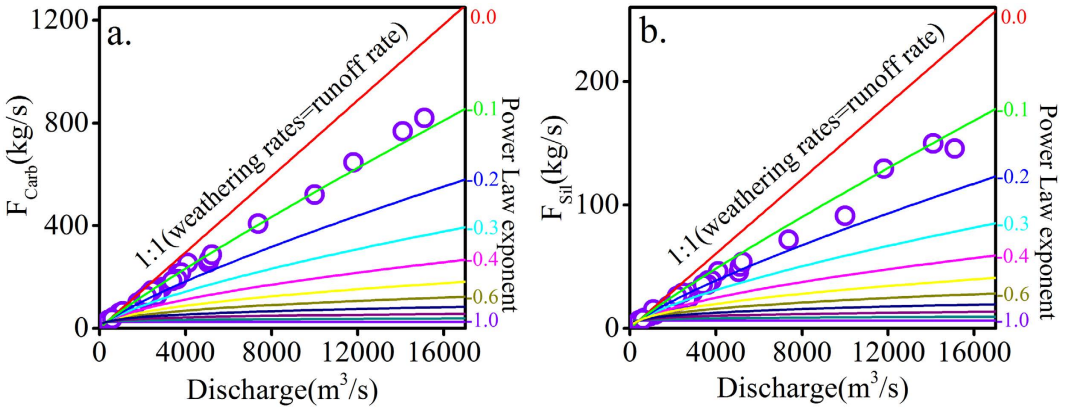

Figure 3. (**a**) Relationship between carbonate weathering fluxes (F_{Carb}) and discharge. (**b**) Relationship between silicate weathering fluxes (F_{Sil}) and discharge.

contribution of silicate mineral dissolution to the dissolved loads changes with discharge, which is similar to the findings of other studies[38,43]. Si, Na^+ and K^+ are from same lithologic source, and variations in $Si/(Na^* + K^+)$ with discharge can be used to interpret the balance between secondary mineral precipitation and primary silicate weathering. The $Si/(Na^* + K)$ ratio can be regarded as a proxy commonly related to the "intensity" of silicate weathering[44].

Because multiple concentration-discharge relationships occur with increasing discharge (Fig. 1), reactive transport can generate various behaviors in the ratio-discharge relationships. The observed variation in $(Na^* + K)/Ca$ with discharge in Wujiang River doesn't show a linear positive relationship or negative relationship. As the mean discharge of the Wujiang River in the monsoon season is approximately 3000 m^3/s, we define that discharge is two times greater than the mean discharge (i.e., 6000 m^3/s) as extremely high discharge. The $(Na^* + K)/Ca$ ratio decreases rapidly with increasing discharge at discharge below 6000 m^3/s (Fig. 2a). Thus, the slope of the $(Na^* + K)/Ca$ ratio-discharge relationship suggests that the relative proportion of solutes derived from silicate weathering decreases with increasing discharge at discharges below 6000 m^3/s. However, $(Na^* + K)/Ca$ has a relative stable value with increasing discharge when the discharge is higher than 6000 m^3/s (Fig. 2a). Under high discharge conditions with short fluid transit times, water cannot reach equilibrium with rocks[14,16]. With increasing discharge, carbonate minerals dissolve rapidly and can drastically alter the water chemistry composition relative to the silicate minerals[14,45]; thus, the $(Na^* + K)/Ca$ ratio decreases with increasing discharge. When discharge is greater than 6000 m^3/s, as most of dissolved solutes concentrations have relative constant values with increasing discharge (Fig. 1), the relative proportion of solutes derived from silicate weathering versus carbonate has a narrow range.

The power law exponent describing the relationship between Si and discharge shows a positive trend (Fig. 1). Dissolved Si concentration is maintained by equilibrium with respect to secondary silicate mineral and the retention of silicate in the reservoir[38,42,43]. The $Si/(Na^* + K)$ ratio increases with increasing discharge for discharge below 6000 m^3/s, suggesting that the relative release of Si to $Na^* + K$ from primary silicates is greater than lower discharge and less dissolved Si is retained in the reservoir with increasing discharge for discharges below 6000 m^3/s. Increasing discharge, decreases the transit time of fluids, leading to less time for the fluids and minerals to reach equilibrium with a secondary Si-bearing phase, and less time for retention in the reservoir in the upper reach. Thus, the $Si/(Na^* + K)$ ratios increase with increasing discharge for discharge below 6000 m^3/s. Extreme discharge will shift deep flow paths to fast near-surface flow paths. Because of the less transit time of water, there is less time for biogeochemical processes such as ions exchange, biological uptake. So the $Si/(Na^* + K)$ ratio is near to the ratio from silicate weathering at extremly high discharge. Therefore, samples show relative stable $Si/(Na^* + K)$ ratios with increasing discharge when the discharge is higher than 6000 m^3/s.

Chemical weathering fluxes affected by hydrological conditions. The temporal variability in discharge on the Yunnan-Guizhou Plateau in southwestern China mainly depends on rainfall associated with the monsoon climate. As discussed above, the major element dynamics are dominated by discharge, and hydrologic flushing further induces chemostatic behavior by increasing the reactive mineral surface area, which accelerates the mineral weathering[38]. In this study, a forward model is used to constrain the elemental sources (Eqs S1–9). Carbonate weathering fluxes (F_{Carb}) and silicate weathering fluxes (F_{Sil}) are calculated using Eqs S11 and 12, respectively.

The results show a broad range: F_{Carb} ranges from 26.1 kg/s to 819.7 kg/s, F_{Sil} varies from 3.7 kg/s to 149.8 kg/s. F_{Carb} and F_{Sil} have strong correlations with discharge (Fig. 3a and b). The strong correlations between chemical weathering fluxes and discharge indicate that chemical weathering is dominated by hydrological conditions. Contours of different power law exponents spanning from dilution (−1) to "chemostasis" (0) (Fig. 3a and b) illustrate the sensitivity of chemical weathering to discharge changes. The power law exponent between F_{Carb} and discharge is approximately −0.1. F_{Sil} has a power law exponent of approximately −0.2 at relatively low discharge rates (e.g., discharge of $<$6000 m^3/s) and approximately −0.1 at extremely high discharge rates (e.g., discharge of $>$6000 m^3/s). Both F_{Carb} and F_{Sil} shows strong chemostatic responses to varying discharge, and F_{Carb} shows

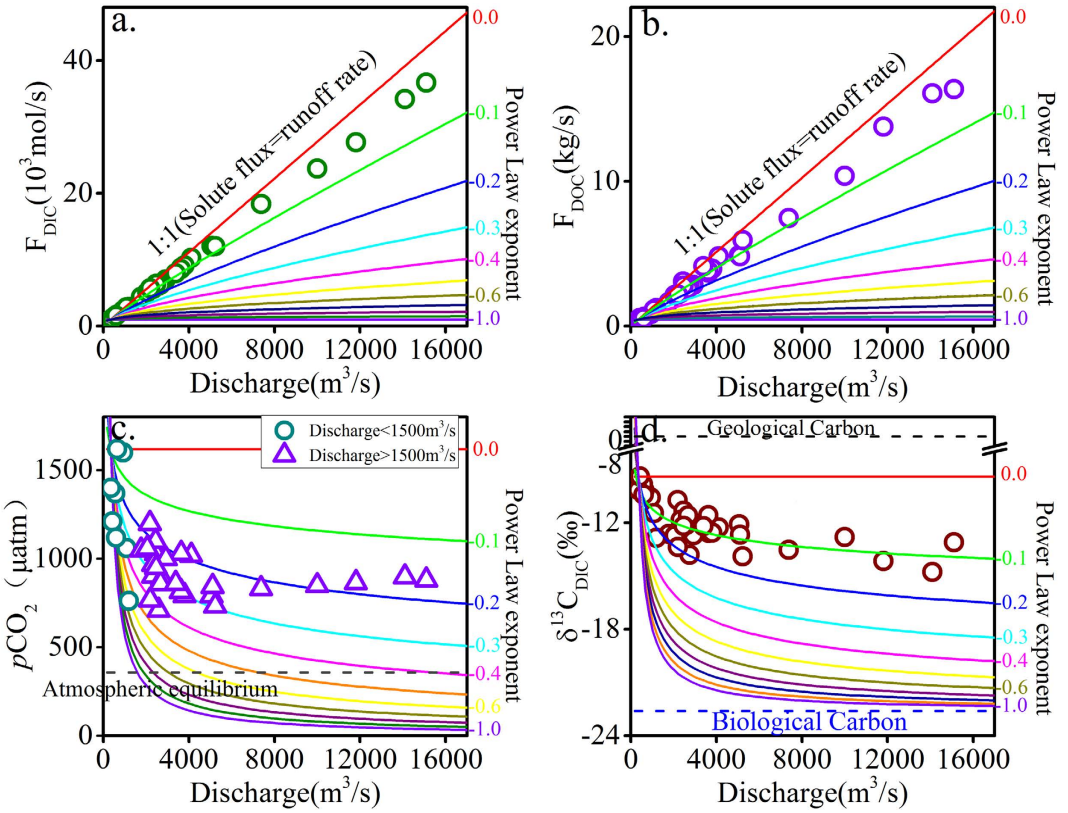

Figure 4. (**a**) Relationship between flux of DIC (F_{DIC}) with discharge. (**b**) Correlation between flux of DOC (F_{DOC}) with discharge. (**c**) Links between pCO_2 and discharge. (**d**) $\delta^{13}C_{DIC}$ values versus increasing discharge.

a slightly more obvious chemostatic response. The near chemostatic behavior of chemical weathering fluxes responding to changing discharge may be ascribed to the hypothesis that fluids will quickly approach chemical equilibrium in rapidly eroding environments[16,43,46]. Variations in chemical weathering fluxes versus discharge can be ascribed to the dissolution kinetics, because the dominance of physical erosion during high discharge allows the more easily weatherable carbonate to dissolve[14]. And Importantly, our results characterize the sensitivity of chemical weathering fluxes to changes in discharge.

Response of dissolved carbon dynamics to hydrological changes. DIC is an important part of the total fluvial carbon to the ocean[47]. DOC is a significant constituent in aquatic ecosystems, and its concentrations in streams is influenced by both temperature and water flow pathway dynamics associated with changes in discharge[48]. The fluxes of DIC (F_{DIC}) and DOC (F_{DOC}) in rivers are strongly linked to climate condition (Fig. 4a and b). As discussed above, DIC and DOC show strong chemostic response with respect to varying discharge. Both F_{DIC} and F_{DOC} have strong positive relationship with discharge (Fig. 4a and b). The chemostic behaviors of DIC should be ascribed to primary production in the basin, as well as dissolution and precipitation. The power law exponents of both F_{DIC} versus discharge and F_{DOC} versus discharge are close to 0, indicating that the fluxes of dissolved carbon in the Wujiang River are dominated by hydrological conditions, and fluxes of DIC and DOC are sensitive to hydrological variability.

Biological CO_2 discharge, *in situ* biodegradation and photosynthesis is the primary driver of the pCO_2 in water[26,30]. Because of the relative low value of DOC and few amounts of aquatic plants in valley type of river channel, the effect of biodegradation and photosynthesis to pCO_2 in the Wujiang river could be neglected. Therefore, biological CO_2 discharge should be the main control on pCO_2, especially during the flooding stage. The values of pCO_2 show a negative correlation with discharge (Fig. 4c) and a power-law dilution effect with increasing discharge. The pCO_2 values exhibit strong chemostatic behavior with respect to increasing discharge when the discharge is greater than 1500 m^3/s. Biological CO_2 produced by microbiologic activities and plant respiration would increase under high temperature conditions in summer at Southwest China[26]. So biological CO_2 discharge is likely responsible for the chemostatic behavior. At extreme discharge rates, the fluid follows near-surface flow paths rather than deep flow paths, and biological CO_2 does not have enough time to react with rocks. Therefore, biological CO_2 can be transported to the river directly, which counteracts the dilution effect following periods of high discharge (Fig. 5). Li *et al.*[26] showed that soil CO_2 plays an important role in shifting $\delta^{13}C_{DIC}$ values in a small karst catchment. Epikarst aquifers water, with more negative $\delta^{13}C_{DIC}$ values than that in riverine water, have an important impact on karstic water carbon in carbonate-rich areas due to the active exchange between the surface water and subsurface flow water. Thus, the water stored in the matrix porosity and soil water with high contents of biological CO_2 would flow into the river induced by high discharge, leading to decrease of $\delta^{13}C_{DIC}$ in the Wujiang

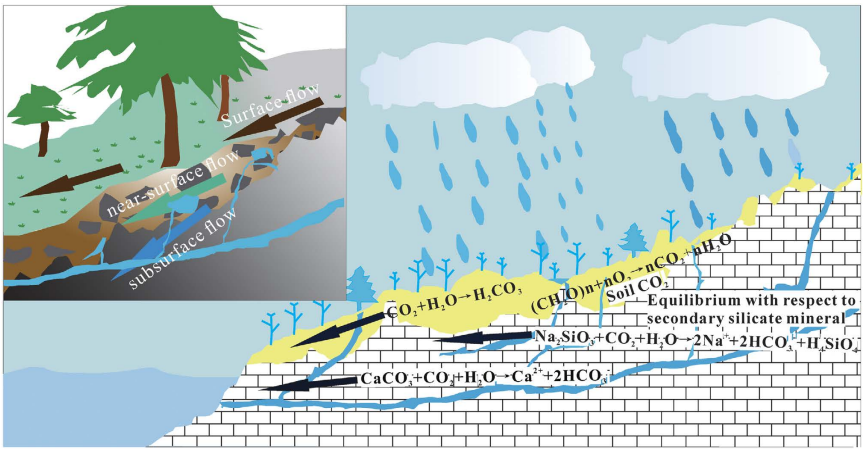

Figure 5. Schematic of chemical weathering and dissolved carbon dynamics in response to changing hydrological conditions in a typical karst catchment. This figure was drawn by software Coredraw X7 (http://www.corel.com/cn/).

River. As indicated in Fig. 4d, there is a generally negative correlation between $\delta^{13}C_{DIC}$ values and discharge. The values of $\delta^{13}C_{DIC}$ in Wujiang River changing with hydrological variability could not be interpreted in terms of simple dilution. Chemical weathering enhanced by increasing discharge produces large amounts of DIC, which is more positive than those of biological CO_2. Thus, the $\delta^{13}C_{DIC}$ does not respond dramatically to the increasing discharge. As seen in Fig. 4d, the $\delta^{13}C_{DIC}$ values exhibit a power-law mixture effect with increasing discharge, indicating that there is a power-law relationship between the $\delta^{13}C_{DIC}$ values and discharge, as follows:

$$\delta^{13}C_{DIC} = aQ^b + c \quad (2)$$

where a, b and c are constants. Usually, c is equal to the $\delta^{13}C$ value of biological CO_2. The exponent in the power-law relationship depends on the amount of biological CO_2. A power law exponent of zero indicates that dilution will not change the values of $\delta^{13}C_{DIC}$ and that biological CO_2 will not be directly discharged into the river under high discharge conditions. A power law exponent close to −1 means that a large amount of biological CO_2 will be discharged into the river, shifting the $\delta^{13}C_{DIC}$ values.

The $\delta^{13}C_{DIC}$ values increase with increased $(Na^* + K)/Ca$ ratios, which represent the relative contribution of silicate weathering versus carbonate weathering (Fig. S4a). The results indicate that silicate weathering is not responsible for the lower values of $\delta^{13}C_{DIC}$ in the high-flow season due to relative low $(Na^* + K)/Ca$ ratios. Thus, more soil CO_2 dissolution following rain water discharge would drop $\delta^{13}C$-DIC value in the river and counteract the riverine pCO_2 at the same time in the high-flow season. There is a positive relationship between $\delta^{13}C_{DIC}$ values and SO_4/DIC ratios (Fig. S4b), suggesting that the lower values of $\delta^{13}C_{DIC}$ are ascribed to the soil CO_2 discharge and the reduced ratio of carbonate weathering by H_2SO_4. In this study, the power law exponent of $\delta^{13}C_{DIC}$ versus discharge is close to −0.1, indicating that relative high carbonate weathering rate and biological CO_2 contribution are stimulated by high discharge likely occurs.

DIC sources. The sources of DIC can be constrained by $\delta^{13}C_{DIC}$ values due to the large difference between biological carbon and geological carbon[1,31,41]. As pCO_2 in riverine water is much higher than pCO_2 in the atmosphere (Fig. 4c), the contribution of atmospheric CO_2 to DIC can be neglected[5,25,30,32,49,50]. Thus, the riverine DIC has two major sources: geological source and biological source. As discussed by Telmer and Veizer[32], carbon isotopes in marine limestones and dolostones deposited since the end of the Proterozoic show typical marine values close to 0‰. C3 plants dominate the study area[25] with the average $\delta^{13}C$ value of −27‰. Cerling *et al.*[51] have reported that there is carbon isotope fractionation of approximately 4.4‰ during the diffusion of CO_2. Therefore, the carbon isotope of soil CO_2 in the Wujiang river basin is likely −22.6‰. Given the different $\delta^{13}C_{DIC}$ of these two endmembers, the source contribution to riverine DIC can be calculated as follows:

$$\delta^{13}C_{DIC} = \delta^{13}C_{geo} \times F_{geo} + \delta^{13}C_{bio} \times \left(1 - F_{geo}\right) \quad (3)$$

where $\delta^{13}C_{geo}$ and $\delta^{13}C_{bio}$ is the $\delta^{13}C$ values of geological carbon and biological carbon, respectively, and F_{geo} is the proportion of carbon from the geological source. In the case that the DIC is affected by carbonate precipitation and CO_2 degassing, the F_{geo} is overestimated because of the isotope fractionation[52].

The contribution of DIC_{bio} (DIC from biological sources) to DIC in river water increases from 41.5% to 65.4% based on the calculation (Eq. 3). Furthermore, the concentrations of DIC_{geo} (DIC from geological sources) and DIC_{bio} can be determined based on the relative proportions of DIC. The DIC_{geo} concentrations show a power-dilution relationship with discharge (Fig. 6a), indicating that DIC_{geo} exhibits strong chemostatic behavior with respect to discharge changes. Increasing carbonate weathering rates are likely responsible for this chemostatic situation. In contrast, DIC_{bio} values show a positive relationship with discharge (Fig. 6b), suggesting that biological DIC influx is the main driver of the chemostic behavior of total DIC with increasing discharge.

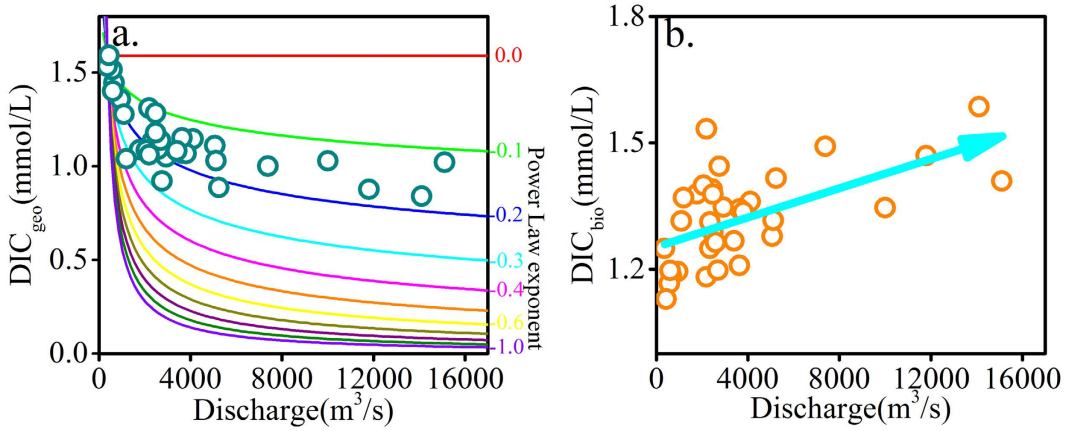

Figure 6. (**a**) Correlation between DIC_{geo} and discharge. (**b**) Correlation between DIC_{bio} and discharge.

Atmospheric precipitation infiltrates into the soil and flush soil CO_2 into the river. Therefore, high discharge brings excessive biological DIC into the river, leading to increasing DIC_{bio} concentrations with increasing discharge.

Fluvial DIC concentrations and $\delta^{13}C_{DIC}$ values primarily reflect the mixing of compositionally distinct end-members (Fig. 6a and b). Physical and biological processed take turns to alter the composition of the DIC pool during changing hydrological conditions (Fig. 5). $\delta^{13}C_{DIC}$ may be more sensitive than DIC concentrations to hydrological changes (Fig. 4a and d), which is in agreement with Waldran *et al.*[53]. Clearly, physical and biological processes affect DIC concentrations during changing hydrological conditions. Therefore, continuous high-frequency monitoring during field programs should be conducted[53]. The results suggest that $\delta^{13}C_{DIC}$ values can be useful for revealing the response of biogeochemical processes to riverine hydrological conditions.

Methods

The study area. The Wujiang River basin (Fig. S5) is located in the center of the Southeast Asian Karst Region, the largest karst area in the world[8,25]. The Wujiang River is the largest tributary on the south bank of the upper Changjiang River, which is the 3rd longest river in the world[8,9]. The drainage area is 87 920 km^2, and the region features a warm subtropical climate[9]. The mean annual precipitation for the last several years has ranged from 850 to 1600 mm[8], and the occurrence of a seasonal monsoon results in high precipitation during summer and low precipitation during winter[10]. Carbonate rocks are widely exposed in this area, with no significant outcrops of evaporites[8].

Sampling and analyses. The sampling site is located at the outlet of the Wujiang River (Fig. S5), where is 45 km away from the mainstream of the Changjiang River. The water samples for chemical and isotopic analyses were collected, monthly, from November 2013 to October 2014, i.e., throughout one entire hydrological year. Additional samples were collected during high-discharge periods. Samples were collected in the middle of the river by boat. pH, teeasured in the field. Alkalinity was determined with 0.02 μM hydrochloric acid mperature(T) and Ec were mwithin 24 hours. The samples were filtered through 0.45 μM cellulose-acetate filter paper. Major cations (K^+, Na^+, Ca^{2+} and Mg^{2+}) and Si were acidified to pH = 2 with ultrapurified HNO_3 and measured via Inductively Couples Plasma-optical Emission Spectrometry (ICP-OES) (with an error of 3%). Anions (SO_4^{2-}, Cl^- and NO_3^-) were analyzed using a Diones ICS90 (with an error of 5%). The DOC was measured using an OI Analytical Aurora 1030 TOC analyzer. For the $\delta^{13}C_{DIC}$ analysis, the method of Li *et al.*[25] was used, with a precision of 0.2%. All these analyses were conducted at the State Key Laboratory of Environmental Geochemistry (Institute of Geochemistry, Chinese Academy of Sciences). Daily water discharge data were obtained online from the Ministry of Water Resources (http://www.hydroinfo.gov.cn/). Finally, pCO_2, SIc and all DIC species were calculated based on mass action relationships and the relative equilibrium constants.

References

1. Khadka, M. B., Martin, J. B. & Jin, J. Transport of dissolved carbon and CO_2 degassing from a river system in a mixed silicate and carbonate catchment. *Journal of Hydrology* **513,** 391–402, doi: 10.1016/j.jhydrol.2014.03.070 (2014).
2. Guo, J., Wang, F., Vogt, R. D., Zhang, Y. & Liu, C. Q. Anthropogenically enhanced chemical weathering and carbon evasion in the Yangtze Basin. *Scientific reports* **5,** 11941, doi: 10.1038/srep11941 (2015).
3. Moquet, J.-S. *et al.* Chemical weathering and atmospheric/soil CO_2 uptake in the Andean and Foreland Amazon basins. *Chemical Geology* **287,** 1–26, doi: 10.1016/j.chemgeo.2011.01.005 (2011).
4. Gaillardet, J., Dupre, B., Louvat, P. & Allegre, C. J. Global silicate weathering and CO_2 consumption rates deduced from the chemistry of large rivers. *Chemical Geology* **159,** 3–30 (1999).
5. Galy, A. & France-Lanord, C. Weathering processes in the Ganges–Brahmaputra basin and the riverine alkalinity budget. *Chemical Geology* **159** (1999).
6. Wu, W., Xu, S., Yang, J. & Yin, H. Silicate weathering and CO2 consumption deduced from the seven Chinese rivers originating in the Qinghai-Tibet Plateau. *Chemical Geology* **249,** 307–320, doi: 10.1016/j.chemgeo.2008.01.025 (2008).

7. Wu, L., Huh, Y., Qin, J., Du, G. & van Der Lee, S. Chemical weathering in the Upper Huang He (Yellow River) draining the eastern Qinghai-Tibet Plateau. *Geochimica et Cosmochimica Acta* **69,** 5279–5294, doi: 10.1016/j.gca.2005.07.001 (2005).
8. Han, G. & Liu, C.-Q. Water geochemistry controlled by carbonate dissolution: a study of the river waters draining karst-dominated terrain, Guizhou Province, China. *Chemical Geology* **204,** 1–21, doi: 10.1016/j.chemgeo.2003.09.009 (2004).
9. Li, C. & Ji, H. Chemical weathering and the role of sulfuric and nitric acids in carbonate weathering: Isotopes (^{13}C, ^{15}N, ^{34}S, and ^{18}O) and chemical constraints. *Journal of Geophysical Research*: *Biogeosciences* **121,** 1288–1305, doi: 10.1002/2015jg003121 (2016).
10. Han, G., Tang, Y. & Xu, Z. Fluvial geochemistry of rivers draining karst terrain in Southwest China. *Journal of Asian Earth Sciences* **38,** 65–75, doi: 10.1016/j.jseaes.2009.12.016 (2010).
11. Kirchner, J. W. & Neal, C. Universal fractal scaling in stream chemistry and its implications for solute transport and water quality trend detection. *Proceedings of the National Academy of Sciences of the United States of America* **110,** 12213–12218, doi: 10.1073/pnas.1304328110 (2013).
12. Hercod, D. J., Brady, P. V. & Gregory, R. T. Catchment-scale coupling between pyrite oxidation and calcite weathering. *Chemical Geology* **151(1–4**), 259–276 (1998).
13. Szramek, K., McIntosh, J. C., Williams, E. L., Kanduc, T., Ogrinc, N. & Walter, L. M. Relative weathering intensity of calcite versus dolomite in carbonate-bearing temperate zone watersheds: Carbonate geochemistry and fluxes from catchments within the St. Lawrence and Danube river basins. *Geochemistry, Geophysics, Geosystems*, **8(4),** doi: 10.1029/2006GC001337 (2007).
14. Tipper, E. *et al.* The short term climatic sensitivity of carbonate and silicate weathering fluxes: Insight from seasonal variations in river chemistry. *Geochimica et Cosmochimica Acta* **70,** 2737–2754, doi: 10.1016/j.gca.2006.03.005 (2006).
15. Ibarra, D. E. *et al.* Differential weathering of basaltic and granitic catchments from concentration–discharge relationships. *Geochimica et Cosmochimica Acta* **190,** 265–293, doi: 10.1016/j.gca.2016.07.006 (2016).
16. Torres, M. A., West, A. J. & Clark, K. E. Geomorphic regime modulates hydrologic control of chemical weathering in the Andes–Amazon. *Geochimica et Cosmochimica Acta* **166,** 105–128, doi: 10.1016/j.gca.2015.06.007 (2015).
17. Raymond, P. A. & Oh, N.-H. Long term changes of chemical weathering products in rivers heavily impacted from acid mine drainage: Insights on the impact of coal mining on regional and global carbon and sulfur budgets. *Earth and Planetary Science Letters*, doi: 10.1016/j.epsl.2009.04.006 (2009).
18. Jiang, Y. J., Wu, Y. X. & Yuan, D. X. Human Impacts on Karst Groundwater Contamination Deduced by Coupled Nitrogen with Strontium Isotopes in the Nandong Underground River System in Yunan, China. *Environmental science & technology* **43,** 7676–7683, doi: 10.1021/es901602t (2009).
19. Voss, B. M. *et al.* Tracing river chemistry in space and time: Dissolved inorganic constituents of the Fraser River, Canada. *Geochimica et Cosmochimica Acta* **124,** 283–308, doi: 10.1016/j.gca.2013.09.006 (2014).
20. Gao, Q. *et al.* Chemical weathering and CO_2 consumption in the Xijiang River basin, South China. *Geomorphology* **106,** 324–332, doi: 10.1016/j.geomorph.2008.11.010 (2009).
21. Amiotte Suchet, P., Probst, J.-L. & Ludwig, W. Worldwide distribution of continental rock lithology: Implications for the atmospheric/soil CO_2 uptake by continental weathering and alkalinity river transport to the oceans. *Global Biogeochemical Cycles* **17,** 1038, doi: 10.1029/2002gb001891 (2003).
22. Li, S. & Bush, R. T. Changing fluxes of carbon and other solutes from the Mekong River. *Scientific reports* **5,** 16005, doi: 10.1038/srep16005 (2015).
23. Bouillon, S. *et al.* Contrasting biogeochemical characteristics of the Oubangui River and tributaries (Congo River basin). *Scientific reports* **4,** 5402, doi: 10.1038/srep05402 (2014).
24. Raymond, P. A. & Cole Jonathan, J. Increase in the export of alkalinity from north america's largest river *Science* (2003).
25. Li, S.-L., Calmels, D., Han, G., Gaillardet, J. & Liu, C.-Q. Sulfuric acid as an agent of carbonate weathering constrained by δ13CDIC: Examples from Southwest China. *Earth and Planetary Science Letters* **270,** 189–199, doi: 10.1016/j.epsl.2008.02.039 (2008).
26. Li, S.-L. *et al.* Geochemistry of dissolved inorganic carbon and carbonate weathering in a small typical karstic catchment of Southwest China: Isotopic and chemical constraints. *Chemical Geology* **277,** 301–309, doi: 10.1016/j.chemgeo.2010.08.013 (2010).
27. León, J. G. & Pedrozo, F. L. Lithological and hydrological controls on water composition: evaporite dissolution and glacial weathering in the south central Andes of Argentina (33°–34°S). *Hydrological Processes* **29,** 1156–1172, doi: 10.1002/hyp.10226 (2015).
28. Voss, B. M. *et al.* Seasonal hydrology drives rapid shifts in the flux and composition of dissolved and particulate organic carbon and major and trace ions in the Fraser River, Canada. *Biogeosciences* **12,** 5597–5618, doi: 10.5194/bg-12-5597-2015 (2015).
29. Hélie, J.-F., Hillaire-Marcel, C. & Rondeau, B. Seasonal changes in the sources and fluxes of dissolved inorganic carbon through the St. Lawrence River — isotopic and chemical constraint. *Chemical Geology* **186,** 117–138 (2002).
30. Barth, J. A. C., Cronin, A. A., Dunlop, J. & Kalin, R. M. Influence of carbonates on the riverine carbon cycle in an anthropogenically dominated catchment basin: evidence from major elements and stable carbon isotopes in the Lagan River (N. Ireland). *Chemical Geology* **200,** 203–216, doi: 10.1016/s0009-2541(03)00193-1 (2003).
31. Rivé, K., Gaillardet, J., Agrinier, P. & Rad, S. Carbon isotopes in the rivers from the Lesser Antilles: origin of the carbonic acid consumed by weathering reactions in the Lesser Antilles. *Earth Surface Processes and Landforms* **38,** 1020–1035, doi: 10.1002/esp.3385 (2013).
32. Telmer, K. & Veizer, J. Carbon fluxes, pCO2 and substrate weathering in a large northern river basin, Canada carbon isotope perspectives. *Chemical Geology* **159** (1999).
33. Godsey, S. E., Kirchner, J. W. & Clow, D. W. Concentration-discharge relationships reflect chemostatic characteristics of US catchments. *Hydrological Processes* **23,** 1844–1864, doi: 10.1002/hyp.7315 (2009).
34. Ryu, J., Lee, K., Chang, H. & Shin, H. Chemical weathering of carbonates and silicates in the Han River basin, South Korea. *Chemical Geology* **247,** 66–80, doi: 10.1016/j.chemgeo.2007.09.011 (2008).
35. Karim, A. & V., J. Weathering processes in the Indus River Basin: implications from riverine carbon, sulfur, oxygen, and strontium isotopes. *Chemical Geology* **170** (2000).
36. Dalai, T. K. *et al.* Major ion chemistry in the headwaters of the Yamuna river system Chemical weathering, its temperature dependence and CO2 consumption in the Himalaya. *Geochimica et Cosmochimica Acta* **66,** 3397–3416 (2002).
37. Millot, R. Northern latitude chemical weathering rates: clues from the Mackenzie River Basin, Canada. *Geochimica et Cosmochimica Acta* **67,** 1305–1329, doi: 10.1016/s0016-7037(02)01207-3 (2003).
38. Clow, D. W. & Mast, M. A. Mechanisms for chemostatic behavior in catchments: Implications for CO2 consumption by mineral weathering. *Chemical Geology* **269,** 40–51, doi: 10.1016/j.chemgeo.2009.09.014 (2010).
39. Basu, N. B. *et al.* Nutrient loads exported from managed catchments reveal emergent biogeochemical stationarity. *Geophysical Research Letters* **37,** L23404, doi: 10.1029/2010gl045168 (2010).
40. Xu, Z. & Liu, C. Chemical weathering in the upper reaches of Xijiang River draining the Yunnan–Guizhou Plateau, Southwest China. *Chemical Geology* **239,** 83–95, doi: 10.1016/j.chemgeo.2006.12.008 (2007).
41. Jin, J., Zimmerman, A. R., Moore, P. J. & Martin, J. B. Organic and inorganic carbon dynamics in a karst aquifer: Santa Fe River Sink-Rise system, north Florida, USA *Journal of Geophysical Research: Biogeosciences* **119,** 340–357, doi: 10.1002/2013jg002350 (2014).
42. Humborg, C., Ittekkot, V., Cociasu, A. & Bodungen, B., V, I., A, C. & von, B. B. Effect of Danube River dam on Black Sea biogeochemistry and ecosystem structure. *Nature* **386,** 385–388 (1997).
43. Maher, K. The role of fluid residence time and topographic scales in determining chemical fluxes from landscapes. *Earth and Planetary Science Letters* **312,** 48–58, doi: 10.1016/j.epsl.2011.09.040 (2011).

44. Moon, S., Huh, Y., Qin, J. & Vanpho, N. Chemical weathering in the Hong (Red) River basin: Rates of silicate weathering and their controlling factors. *Geochimica et Cosmochimica Acta* **71,** 1411–1430, doi: 10.1016/j.gca.2006.12.004 (2007).
45. Wei, G. *et al.* Seasonal changes in the radiogenic and stable strontium isotopic composition of Xijiang River water: Implications for chemical weathering. *Chemical Geology* **343,** 67–75, doi: 10.1016/j.chemgeo.2013.02.004 (2013).
46. Maher, K. & Chamberlain C. P. Hydrologic regulation of chemical weathering and the geologic carbon cycle. *Science* **343(1502),** doi: 10.1126/science.1250770 (2014).
47. Meybeck, M. Riverine transport of atmospheric carbon: sources, global typology and budget. *Water Air Soil Pollut* **70,** 443–463 (1993).
48. Winterdahl, M., Laudon, H., Lyon, S. W., Pers, C. & Bishop, K. Sensitivity of stream dissolved organic carbon to temperature and discharge: Implications of future climates. *Journal of Geophysical Research: Biogeosciences* **121,** 126–144, doi: 10.1002/2015jg002922 (2016).
49. Aucour, A.-M., Sheppard, S. M. F., Guyomar, O. & Wattelet, J. Use of ^{13}C to trace origin and cycling of inorganic carbon in the Rhône river system. *Chemical Geology* **159,** 87–105, doi: http://dx.doi.org/10.1016/S0009-2541(99)00035-2 (1999).
50. Mayorga, E. *et al.* Young organic matter as a source of carbon dioxide outgassing from Amazonian rivers. *Nature* **436,** 538–541, doi: 10.1038/nature03880 (2005).
51. Cerling, T. E., Solomon, D. K., Quade, J. & Bowman, J. R. The Macalpine Hills Lunar Meteorite ConsortiumOn the isotopic composition of carbon in soil carbon dioxide. *Geochimica et Cosmochimica Acta* **55,** 3403–3405, doi: http://dx.doi.org/10.1016/0016-7037(91)90498-T (1991).
52. Frondini, F. *et al.* Carbon dioxide degassing from Tuscany and Northern Latium (Italy). *Global and Planetary Change* **61,** 89–102, doi: 10.1016/j.gloplacha.2007.08.009 (2008).
53. Waldran, S., Scott, E. M. & Soulsby, C. Stable Isotope Analysis Reveals Lower-Order River Dissolved Inorganic Carbon Pools Are Highly Dynamic. *Environ. Sci. Technol.* **41,** 6156–6162 (2007).

Acknowledgements

This work is financially supported by National Natural Science Foundation of China (Grant Nos. 41422303, 41571130072 and 41130536) and the Ministry of Science and Technology of China through Grant Nos. 2016YFA0601000 and 2013CB956700.

Author Contributions

Si-Liang Li designed the research, Jun Zhong conducted the field sampling, analyzed the samples, Si-Liang Li and Jun Zhong drafted the manuscript, Faxiang Tao, Fujun Yue and Cong-Qiang Liu contributed to the results discussion and the manuscript modification.

Additional Information

Supplementary information accompanies this paper at http://www.nature.com/srep

Competing financial interests: The authors declare no competing financial interests.

How to cite this article: Zhong, J. *et al.* Sensitivity of chemical weathering and dissolved carbon dynamics to hydrological conditions in a typical karst river. *Sci. Rep.* **7**, 42944; doi: 10.1038/srep42944 (2017).

Publisher's note: Springer Nature remains neutral with regard to jurisdictional claims in published maps and institutional affiliations.